Monaldi Archives for Chest Disease

eISSN 2532-5264 https://www.monaldi-archives.org/

Monaldi Arch Chest Dis 2026 [Online ahead of print]

To cite this Article:
Manzari Tavakoli G, Mazraehei Farahani M, Moradhaseli Z, et al. **A pilot animal study of a novel nanocomposite silicone airway stent: biocompatibility and performance in a sheep model**. *Monaldi Arch Chest Dis* doi: 10.4081/monaldi.2026.3840

Submitted: 4-12-2025
Accepted: 9-03-2026

A pilot animal study of a novel nanocomposite silicone airway stent: biocompatibility and performance in a sheep model

Gita Manzari Tavakoli,[1] Maryam Mazraehei Farahani,[2,3] Zahra Moradhaseli,[4] Arda Kiani,[5] Hossein Kazemizadeh,[6] Abdol-Mohammad Kajbafzadeh[1]

[1]Pediatric Urology and Regenerative Medicine Research Center, Children's Medical Center, Gene, Cell and Tissue Research Institute, Tehran University of Medical Sciences; [2]Farhikhtegan Medical Convergence Sciences Research Center, Farhikhtegan Hospital Tehran Medical Sciences, Islamic Azad University, Tehran; [3]Clinical Tuberculosis and Epidemiology Research Center, National Research Institute of Tuberculosis and Lung Diseases, Shahid Beheshti University of Medical Sciences, Tehran; [4]School of Mechanical Engineering, College of Engineering, University of Tehran; [5]Lung Research and Developmental Center, Shahid Beheshti University of Medical Sciences, Tehran; [6]Department of Pulmonary Medicine, Faculty of Medicine, Tehran University of Medical Sciences, Tehran, Iran

Correspondence: Maryam Mazraehei Farahani, Farhikhtegan Medical Convergence Sciences Research Center, Farhikhtegan Hospital Tehran Medical Sciences, Islamic Azad University, Tehran, Iran.
Tel.: +9821-44867262. Fax: +9821-44845171. E-mail: maryam.m.farahani87@gmail.com

Contributions: Abdol-Mohammad Kajbafzadeh, Maryam Mazraehei Farahani: study conception, design, and supervision. Zahra Moradhaseli, Arda Kiani, Hossein Kazemizadeh: material preparation. Gita Manzari Tavakoli: first draft of the manuscript. Gita Manzari Tavakoli, Maryam Mazraehei Farahani: editing and reviewing. All authors read and approved the final manuscript.

Conflict of interest: the authors declare no potential conflict of interest.

Ethics approval and consent to participate: the approved principles for working with laboratory animals were observed according to the guidelines issued by the Research Ethics Committee of Imam Khomeini Hospital Complex—Tehran University of Medical Sciences, Approval ID: IR.TUMS.IKHC.REC.1401.032, Tehran, Iran.

Availability of data and materials: the data that support the findings of this study are available on request from the corresponding author. The data are not publicly available due to privacy or ethical restrictions.

Acknowledgments: the authors would express their sincere gratitude to Dr. Kajbafzadeh for kindly providing the laboratory facilities and support that made this research possible.

Abstract

Airway obstruction resulting from both malignant and non-malignant etiologies is a growing challenge in pulmonary diseases and critical care medicine, particularly after the COVID-19 pandemic. Conventional silicone and metallic airway stents may be indicated in airway obstructions that lead to palliative relief, but they may lead to complications such as migration, inflammatory reaction to the adjacent tissue, and granulation tissue overgrowth. We conducted this animal pilot study to investigate the biocompatibility of a next-generation nanocomposite silicone airway stent, engineered with 3wt% hydrophobic nano-silica reinforcement. Innovative characteristics of the stent include improved biocompatibility and reduced mucus adhesion due to its hydrophobic properties. A refined stenting technique was applied to implant the stent in the trachea of two sheep models by assembling two endotracheal tubes, Ambu, and the stent. After a two-month follow-up, high-resolution computed tomography imaging, 3D virtual bronchoscopy, bronchoscopy, and biopsy of the tracheal wall were done. Histopathologic assessment demonstrated an inflammatory infiltrate dominated by lymphocytes, without stromal reactions, mucosal and submucosal thickening, or granulation, confirming a favorable tissue tolerance. These preliminary outcomes emphasize the stent's potential as a transformative therapeutic option; however, the study's limited sample size and absence of comparative controls highlight the necessity for further preclinical trials with quantitative airflow parameters to elucidate the clinical translatability of this innovative biomaterial solution for airway obstructions. Additionally, the findings of this study can address the unmet needs in managing complex airway obstructions, particularly for patients refractory to current therapeutic options in the future.

Key words: nanocomposite silicone stent, airway stent, pilot animal study, hydrophobic nano-silica, sheep trachea.

Introduction

Airway obstruction is an anatomic narrowing or occlusion that decreases the ability to exchange air properly in and out of the lungs. The prevalence of airway obstruction is reported to be around 10% in a community-based sample of adults according to the American Thoracic Society (ATS) criteria [1]. However, due to the COVID-19 pandemic, a growing number of patients who have been extubated suffer from airway obstruction caused by tracheal stenosis resulting from prolonged intubation [2]. Airway obstruction may result from different factors, including malignant and non-malignant causes [3,4]. Malignant causes include direct involvement of the airway by bronchogenic carcinoma, by extension of esophageal or thyroidal carcinomas, or by metastasis [3]. External compression of the airway by enlarged lymph nodes can also lead to central airway obstruction [3]. Non-malignant causes are mainly due to post-intubation or post-tracheostomy stenosis, tracheomalacia, foreign bodies, benign endobronchial tumors, infectious, systemic, or autoimmune diseases, post-lung transplant stenosis, radiation lesions, esophagorespiratory fistulas, or idiopathic tracheal stenosis [4].

In recent decades, airway stenting, also known as endobronchial prosthesis, has been investigated as an emerging treatment for airway obstruction. Most of the obstructions may benefit from multimodality palliative approaches, such as stenting, if they remain surgically incurable [3]. Stenting is indicated for extrinsic compression, residual obstruction after thermal therapy, mixed endobronchial and extrinsic tumors, cartilage loss from tumor destruction, or malignant tracheoesophageal fistula [5]. Also, stenting is indicated by strictures or stenosis longer than 4 cm, inoperable benign obstructions, post-transplant airway stenosis, tracheobronchomalacia as a trial before tracheoplasty, and benign tracheoesophageal fistulas [5].

Notably, stents made of different materials may cause inflammatory reactions in the adjacent tissue, mucus compaction, granulation, and displacement, which raises concerns about this intervention [6,7]. Based on the material compositions, different types of airway stents are silicone, bare metallic, and hybrid stents [8]. Silicon rubbers are polymers based on silicon, which exhibit various features including heat, wear, and flame resistance, transparency, gas permeability, chemical stability, and electrical insulation, in addition to hydrophobicity that shows minimal reaction to body fluids and reduction in the mucin adhesion and mucus plugging. However, pure silicone demonstrates insufficient mechanical features due to inadequate interaction and flexibility in the silicone matrix [9-11]. Silicone can be reinforced with various nanoparticles, such as silica, montmorillonite (MMT), and titanium oxide, to improve their mechanical, hydrophobic properties, and biocompatibility [12]. Silica nanoparticles have gained

the attention of researchers due to their unique features for in vivo applications, good biocompatibility, and enhancement of the mechanical and hydrophobic properties of silicone/silica nanocomposites [13]. Adding nano-silica, as an inorganic nanoparticle, can enhance the Shore A hardness, tensile strength, and tear limit of silicone rubber, thereby improving the mechanical features of the silicone matrix [10,14,15]. However, the usage of nanoparticles leads to a reduction in transparency and an increase in viscosity [9]. Moreover, nanoparticles can change the surface roughness and hydrophobic properties [2].

The silicone stents used in this pilot study were manufactured by adding 3wt% nano-silica to the silicone matrix, a formulation that was previously shown to reinforce the mechanical properties of silicone in our earlier study [2]. Among different percentages of nanoparticles, adding 3wt% hydrophobic nano-silica leads to uniform distribution throughout the silicone matrix. We aim to conduct an animal pilot study to evaluate the histocompatibility of the stents in two bred sheep's trachea after a two-month follow-up.

Materials and Methods

Stent preparation

The silicone stent design was the classical stent proposed by Jean-François Dumon [16]. The dimensions of the stents were 5 cm in length, 20 mm in diameter, and 1.5 mm in thickness (Figure 1A). Increasing the concentration of hydrophobic nano-silica particles above a threshold would significantly increase the viscosity of emulsions and decrease the precision and quality of the molding process [2]. Moreover, the hydrophobic properties of the stent led to a decrease in plaque mucus in the tubular stent. Silicone airway stents were reinforced with hydrophilic nano-silica (NANO Company, Made in the United States), with a particle size of 20-35 nm. The selection of this particle size range was based on a previous study demonstrating that nano-silica particles in the 7–40 nm range significantly enhanced polymer properties [17]. Particles with an average size of approximately 20 nm, in particular, showed a high specific surface area, promoting stronger filler–matrix interactions and leading to improved ultimate strength, fracture toughness, and elongation at break of the composite [2]. Stents were prepared with silica concentrations of 3 wt% and room temperature vulcanizing-2 (RTV-2) silicone polymer (NuSil-Avantor Company, Made in the United States), which has a 40 Shore A hardness. Before molding, the two RTV-2 silicone/silica components were mixed in equal portions and kept in a vacuum chamber to have a bubble-free emulsion (Figure 1A).

The molding and curing procedures were the final steps for manufacturing the stents. To calculate the surface free energy, the contact angle of diiodomethane was measured as a nonpolar liquid. Adding 3wt% hydrophobic silica nanoparticles resulted in a slight change in the contact angle. The dispersion status of silica in the nanocomposites was evaluated by Scanning Electron Microscope (SEM) (MIRA3 TESCAN, MT-CH 502.06, Made in the Czech Republic) images, as shown in Figure 1B. SEM images confirmed that silica nanoparticles were homogeneously dispersed and distributed throughout the silicone matrix [2]. Also, the radial force of the nano-silica-reinforced stents was 10% more than that of pure silicone stents [2].

Pilot animal study

As a pilot study, only two sheep were used, and planning for further studies with more samples is considered in the future. A comparative control group with stents such as conventional silicone or metallic airway stents was not included in this study due to the focus, which was primarily on the initial feasibility and safety assessment of the new stent design, as well as limitations in our available resources.

Two Female genetically modified and certified sheep were prepared from a modern industrial livestock facility equipped with surveillance cameras and attended by a full-time veterinarian, and then transported to the animal house of the Tehran University of Medical Sciences. The two heterozygous Afshar sheep, which were 10 months old and weighed approximately 70 kg each, were used in this animal study (Figure 2A). Among laboratory animals, sheep's long neck provides an extended airway anatomy that allows for more evaluation of tracheal interventions. Therefore, given the similarity and complexity of the sheep trachea to that of humans, sheep are considered an ideal animal model for conducting pulmonary stent tests in the animal pilot phase [18,19]. The veterinarian examined the sheep before the procedure. The sheep received the necessary vaccine according to the schedule three months before the stenting (FMD on December 4, 2021, Pasteurellosis on September 19, 2021, Vira-Peste on September 6, 2021, Brucella on August 29, 2021, Varicella on March 31, 2021, Agalactia on April 28 2021, Syva-Bax on March 15, 2022, Syva-Bax on February 7, 2022). Also, the sheep were sheared and washed with anti-tick shampoo to prevent the transmission of Crimean–Congo hemorrhagic fever (CCHF) disease. Screening for the absence of hydatid cysts was also performed.

An experienced surgical team, certified in the principles of care and use of laboratory animals, was to perform and supervise the stenting procedure (Figure 2B). The animal surgery room was equipped with all the necessary facilities for administering appropriate anesthesia, including an

animal ventilator, a cold light source, and an Ambu bronchoscope (Ambu® aView™, 405002000, Made in Taiwan) (Figure 2B). Before the stenting, airway mucosal anesthesia was administered by the veterinary anesthesiologist to ensure that the sheep would not experience any pain or distress during the procedures. In each phase of this animal study, the approved principles for working with laboratory animals were observed according to the guidelines issued by the Research Ethics Committee of Imam Khomeini Hospital Complex—Tehran University of Medical Sciences, Approval ID: IR.TUMS.IKHC.REC.1401.032, Tehran, Iran.

Stenting technique

A practical and straightforward method with no limitations, such as the size or diameter of the rigid tools, was used in which stent placement, repositioning, and rotation could be easily performed in sheep [20]. However, this technique should be modified for implantation in human stenotic tracheal or bronchial segments due to stent compression through regions with a significantly reduced lumen. Two size 8.5 endotracheal tubes were connected and assembled to get longer tubes. The cuff of the first endotracheal tube was suctioned, and the stent was placed around the cuff of the second one. Then, the distal balloon of the silicone stent was inflated, located at the end of the endotracheal tube, to stabilize the stent during transfer into the trachea [20] (Figure 2 C-E).

For simple stenting, a Xylocaine 2% Jelly was rubbed around the balloon surface. Stenting began with tracheal bronchoscopy to localize the target area. After the stent is placed at the desired location, the balloon is deflated and the stent is positioned in the target position. An Ambu bronchoscope was used to observe the stents. The large-sized Ambu tube was guided through the endotracheal tube, with some Xylocaine 2% Jelly applied to the endotracheal tube for improved movement of the Ambu. Due to the flexibility of the endotracheal tube, Ambu can also guide the tube. A bronchoscopy was immediately performed to confirm the position and condition of the stents, demonstrating proper stent positioning and well-placed to the tracheal wall (Figure 3A and B).

After successful stenting, both sheep were kept in the animal house, where they underwent clinical examinations twice daily for two-month follow-up by the on-site veterinarian.

Evaluation of outcomes

Outcomes of the study were clinical tolerance, position fit of the stent, and histological biocompatibility. Clinical tolerance of stents was evaluated by using a standardized scoring

system, shown in *Supplementary Table 1*, during a predefined follow-up period of 60 days after the procedure. Both sheep were monitored from the immediate post-procedural period until sacrifice at day 60, by the on-site veterinarian. The veterinarian examined both sheep twice daily at 10 am and 10 pm for two-month follow-up to score the following criteria: posture, alertness, appetite, pain symptoms, respiration, and temperature. Scores ranged from 1 to 5, yielding a maximum total of 30 at each assessment timepoint, with higher scores indicating better and lower scores indicating poorer clinical findings. Additional diagnostic findings or comments were also recorded.

To assess the position fit of stent, both sheep were transferred to the Animal Laboratory Department, and a bronchoscopy was performed. The tracheobronchial tree can be visualized and reconstructed by using Virtual Bronchoscopy (VB). VB, as a non-invasive technique, is based on computed tomography (CT) scans to create high-resolution three-dimensional (3D) images down to the sixth or seventh bronchial subdivision, quantitatively measuring the geometry of the trachea and its branches, as well as the bronchial orifices [21].

The histological evaluation was performed following a standardized scoring system, as shown in *Supplementary Table 2*, using Histology Pathology Lab Microscope (SUNNY, NE-600, Made in China) at the Pathology and Immunohistochemistry Laboratory at the Imam Khomeini Hospital Complex (Tehran University of Medical Sciences). Treated tracheal sections were compared with untreated areas distal to the stent. Sections were evaluated for biocompatibility by semi-quantitatively assessing inflammatory cell infiltration—including polymorphonuclear cells, lymphocytes, plasma cells, and macrophages—as well as the presence of necrosis. Tissue reactions such as stromal reaction, mucosal or submucosal thickening, and granulation tissue were also analyzed.

Results

Clinical tolerance

According to the standardized scoring system, both sheep had symptoms of reduced appetite and pain, receiving a score of 3 out of 5 during the first two days after stent placement. However, their appetite and pain improved at day 3, and neither animal showed symptoms of clinical intolerance throughout the observation period; thus, the sheep could finish the observation period. All the clinical symptoms are shown *Supplementary Table 1*.

CT scans, 3D-virtual bronchoscopy

As shown in Figure 3 C-F, CT scans reveal a linear radiolucent structure within the trachea at the level indicated by the blue arrow, corresponding to the nanocomposite silicon airway stent. The stent appears well-positioned along the middle posterior tracheal wall. The tracheal lumen is maintained with no evidence of collapse, displacement, or significant obstruction adjacent to the stent. The surrounding tracheal structures are preserved, and there is no evidence of surrounding mass or extrinsic compression on the trachea. 3D VB demonstrates the endoluminal view with a patent airway, and the stent maintains a luminal structure. The tracheal walls are smooth, suggesting a proper stent expansion interface between the airway and the stent's surface. There are no signs of significant obstruction, granulation tissue, or mucosal irregularity. Tracheal bifurcation (carina) is visualized distally, confirming that the stent does not obstruct distal airways. Both CT and virtual bronchoscopy confirm adequate positioning and functional outcome post-stenting, with the airway lumen remaining open and structurally supported.

The stent site after the two-month follow-up is shown in Figure 3G and H. Multiple superficial erosions were present at the stent site. These erosions with irregular red borders are on the mucosal surface around the lumen, caused by friction or pressure from the stent. Therefore, a biopsy sample was taken from the erosion at the stent site in the trachea of the sheep. Then, samples were fixed in 10% Neutral buffered formalin (NBF) and sent to the pathology laboratory.

Histological biocompatibility

Generally, there was slight tissue reaction to the stent as compared to the untreated areas distal to the stent. Histopathologic evaluation of tissue taken from the stent site of the trachea shows that the submucosa of the bronchioles is filled with inflammatory cells (Figure 4). Lymphocytes are the predominant cells, with plasma cells and macrophages also present. There is no stromal reaction, mucosal and submucosal thickening, and granulation. A reaction to a foreign body cannot be detected in the biopsies, confirming a favorable tissue tolerance. Detailed scoring of histological biocompatibility is shown *Supplementary Table 2*. Each score shows the mean value for the entire sample and should be interpreted in the context of the localized changes that contributed to the higher average score, even though the overall appearance and tissue reaction remained tolerable.

Discussion

In this animal pilot study, a nanocomposite silicone airway stent was implanted which was reinforced with 3wt% hydrophobic nano-silica nanoparticles and RTV-2 silicone polymer using a modified technique that allowed for a practically controlled placement of the stent. Microscopic examination revealed an inflammatory reaction, with no evidence of stromal reaction, mucosal and submucosal thickening, granuloma formation, or foreign body reaction, indicating good biocompatibility in the short term. Comparing different types of stent composition, conventional silicone stents may migrate within the airway tissue and potentially induce a reaction in the airway mucosa, resulting in accumulation and occlusion [22]. Additionally, the fixed diameter of the silicone stents makes them unsuitable for unusual airway anatomies, which can lead to the collapse of some bronchi [22]. Metal airway stents may cause infectious complications and metal mesh breakage in the long term [22]. Additionally, the Food and Drug Administration (FDA) does not recommend the use of metallic stents unless no suitable alternative airway stents are available for benign obstructions [23]. Generally, rigid bronchoscopes are widely used in performing stenting by applying mechanical pressure to a folded stent in the rigid [24]. However, the usage of rigid bronchoscopy may be limited due to the rigid's size, length, and inner diameter in addition to contraindications such as presence of cervical spine injury, airway or maxillofacial trauma, patient with aneurysm of the aorta, and contraindications for general anesthesia [25,26]. Therefore, an innovative procedure for stenting was applied by assembling two endotracheal tubes, Ambu, and the stent, which eliminates the need for rigid bronchoscopes [20]. However, this technique is not routinely employed in clinical practice and should be modified for implantation in human stenotic tracheal or bronchial segments. The findings of this study, along with the new stenting technique, will help in conducting well-designed animal studies.

The use of sheep as an animal model for tracheal stenting is recommended due to their similar size to humans [27]; therefore, we have chosen sheep for our experiment to study the designed stents. Other animal pilot studies have been recently conducted to evaluate the newly developed airway stents in the treatment of tracheal stenosis. In our pilot study, a hydrophilic nano-silica silicone airway stent was used with a 40 Shore of A hardness. Increasing Shore A hardness, a silicone stent with 70-75 Shore A hardness and radiopaque barium sulfate was developed in a normal canine trachea [28]. The stent had a corrugated external surface with discontinuous and protruding arcs, a highly polished inner surface, and smooth extremities that resembled the tracheobronchial rings. After a two-month follow-up, the stent was well-positioned and

biocompatible in the canine trachea and a mild submucosal inflammatory infiltrate was observed, accompanied by scattered granulation tissue, vascular neoformation, and the absence of microorganisms. The epithelial basal membrane was well-preserved [28]. In another pilot study, GINA stent, a radiopaque silicone airway stent, demonstrated good mechanical properties in a pig tracheal stenosis model [29]. This stent was characterized by an anti-migration design, a flexible and dynamic structure, and radiopacity achieved through the use of barium sulfate, which facilitates stent tracking. Neither mucus retention nor granulation tissue formation was observed during the short-term (3 weeks) follow-up. However, stent migration was observed in one of the four pigs with the GINA stent [29]. Moreover, a self-expandable polyurethane-covered stent was developed and placed in the trachea of Wistar rats [30]. This stent was made of nitinol mesh woven from a single strand and covered with polyurethane membrane. It demonstrated biocompatibility with the trachea, with no evidence of adherence of the stent to the tracheal mucosa. However, there was no difference in tracheal wall injuries, granulation tissue, inflammatory activity, and dilatation between the polyurethane-covered and non-covered stents [30]. In another animal pilot study, a bioresorbable tracheal stent, made of poly (D, L-lactide-co-ε-caprolactone) metacrylates, was developed for use in a tracheal stenosis model of New Zealand White rabbits [31]. The stents demonstrated minimal migration, acceptable biocompatibility, and good clinical tolerance, which was because of the helix-shaped surface structure [31].

Regarding late complications such as granulation tissue formation, tumor regrowth, stent migration, and difficult stent removal, several innovative solutions have been addressed [32]. To prevent granulation tissue formation, several studies developed drug-eluting tracheal stents that release agents such as sirolimus [33], paclitaxel [34], ciprofloxacin [35], doxycycline [36], and vancomycin [37]. These agents decrease the release of inflammatory cytokines and prevent the proliferation of fibroblasts and bacterial colonization. Also, I^{125}-loaded radioactive tracheal stents can avoid the regrowth of tumors in stenosis due to malignant airway obstruction [38]. To prevent difficult stent removal, biodegradable stents made of polydioxanone [39], silk fibroin-PCL [40], poly (lactic-co-glycolic acid) with polyisoprene [41], or magnesium alloys [42] have been developed. To prevent stent migration due to anatomical mismatch, 3D-printing stents with balanced mechanical properties is used to fabricate patient-specific tracheal stents, improving mechanical matching [43].

Despite the promising results, limitations were not precluded in this study. The number of animals was limited to only two, which could prevent the generalizability of the results. However, this was a pilot study, and planning for further studies with more samples was considered. Also, the

study was conducted exclusively in healthy sheep without airway stenosis–related anatomical alterations; therefore, the translational relevance of the proposed stenting technique to clinically stenosed airways may be limited in disease-specific models. The study did not include a comparative control group using conventional silicone or metallic airway stents due to the focus on the initial feasibility and safety assessment of the new stent, in addition to limitations in our available resources. The absence of a control group also prevented a direct comparison of the tissue reactions and biocompatibilities, which made it challenging to attribute the results solely to the nanocomposite formulation. Moreover, the presence of necrosis in some biopsies needed further histological assessment to determine whether this represented a localized injury, procedural artifact, or a material-related effect. Additionally, there was a lack of quantitative evaluation of functional outcomes such as airflow dynamics and mucus accumulation. Future studies should incorporate functional airflow assessments (e.g., quantitative airflow volume or airway resistance), mechanical assessments (e.g., migration testing), and head-to-head comparisons with conventional silicone and metal stents to evaluate clinical translatability.

Conclusions

This pilot study evaluates the feasibility and short-term biocompatibility of an innovative nanocomposite silicone airway stent reinforced with 3wt% hydrophobic nano-silica in the sheep model. Histopathological analysis revealed a lymphocyte-predominant inflammatory reaction, devoid of stromal reaction, mucosal and submucosal thickening, or granulomatous reactions, emphasizing its favorable biocompatibility profile. Also, reliable maintenance of airway patency was achieved without evidence of migration or significant tissue compromise. The findings of this study, along with the new stenting technique, will help in conducting well-designed animal studies.

References

1. Shin C, In KH, Shim JJ, et al. Prevalence and correlates of airway obstruction in a community-based sample of adults. Chest 2003;123:1924-31.
2. Morad Hasely Z, Farahani MM, Baniassadi M, et al. Design and fabrication of silicone-silica nanocomposites airway stent. Front Mater 2023;10:1114981.
3. Folch E, Keyes C. Airway stents. Ann Cardiothorac Surg 2018;7:273-83.
4. Barros Casas D, Fernandez-Bussy S, Folch E, et al. Non-malignant central airway obstruction. Arch Bronconeumol 2014;50:345-54.

5. Labaki W, Ortiz R, Khalil S, et al. Endobronchial stent indications, types, postinsertion complications, and therapeutic interventions in malignant and nonmalignant airway obstruction. Chest 2014;146:748A.
6. Mathisen DJ, Morse CR. Master techniques in surgery: thoracic surgery: lung resections, bronchoplasty, 1e. Philadelphia, PA, USA: Lippincott Williams & Wilkins; 2015:.
7. Freitag L, Eicker R, Linz B, Greschuchna D. Theoretical and experimental basis for the development of a dynamic airway stent. Eur Respir J 1994;7:2038-45.
8. Liu L, Kong J, Georg C. Recent advances in airway stenting. Shanghai Chest 2020;4:6.
9. Moretto HH, Schulze M, Wagner G. Silicones. In: Ullmann's Encyclopedia of Industrial Chemistry. Hoboken, NJ, USA: Wiley VCH.
10. Wu L, Wang X, Ning L, et al. Improvement of silicone rubber properties by addition of nano-SiO2 particles. J Appl Biomater Funct Mater 2016;14:e11-4.
11. Ji J, Ge X, Pang X, et al. Synthesis and characterization of room temperature vulcanized silicone rubber using methoxyl-capped MQ silicone resin as self-reinforced cross-linker. Polymers 2019;11:1142.
12. Liu J, Yao Y, Chen S, et al. A new nanoparticle-reinforced silicone rubber composite integrating high strength and strong adhesion. Compos A Appl Sci Manuf 2021;151:106645.
13. Kim M, Park JH, Jeong H, et al. An evaluation of the in vivo safety of nonporous silica nanoparticles: ocular topical administration versus oral administration. Sci Rep 2017;7:8238.
14. Zayed SM, Alshimy AM, Fahmy AE. Effect of surface treated silicon dioxide nanoparticles on some mechanical properties of maxillofacial silicone elastomer. Int J Biomater 2014;2014:750398.
15. Yan F, Zhang X, Liu F, et al. Adjusting the properties of silicone rubber filled with nanosilica by changing the surface organic groups of nanosilica. Compos B Engin 2015;75:47-52.
16. Dumon JF. A dedicated tracheobronchial stent. Chest 1990;97:328-32.
17. Sohrabi KL, Zolriasatein A, Eftekhari YB. Effect of silica nanoparticles modified with different concentrations of stearic acid on microstructure, mechanical & electrical properties of RTV-2 silicone rubber nanocomposite. J Med Nanomater Chem 2023;5:16-32.
18. Banstola A, Reynolds JNJ. The sheep as a large animal model for the investigation and treatment of human disorders. Biology 2022;11:1251.
19. De Las Heras Guillamón M, Clau LB. The sheep as a large animal experimental model in respiratory diseases research. Arch Bronconeumol 2010;46:499-501. [Article in Spanish].

20. Mazraehei Farahani M, Kajbafzadeh AM, Kiani A, et al. Developing an innovative interventional approach for stenting trachea. BMJ Surg Interv Health Technol 2025;7:e000180.
21. Horton KM, Horton MR, Fishman EK. Advanced visualization of airways with 64-MDCT: 3D mapping and virtual bronchoscopy. AJR Am J Roentgenol 2007;189:1387-96.
22. Puma F, Farabi R, Urbani M, et al., Long-term safety and tolerance of silicone and self-expandable airway stents: an experimental study. Ann Thorac Surg 2000;69:1030-4.
23. Aravena C, Gildea TR. Advancements in airway stents: a comprehensive update. Curr Opin Pulm Med 2024;30:75-83.
24. Yim APC, Abdullah V, Izzat MB, et al. Video-assisted interventional bronchoscopy. Surgical Endoscopy 1998;12:444-7.
25. Batra H, Yarmus L. Indications and complications of rigid bronchoscopy. Expert Rev Respir Med 2018;12:509-20.
26. Nomori H, Horio H, Suemasu K. Bougienage and balloon dilation using a conventional tracheal tube for tracheobronchial stenosis before stent placement. Surg Endosc 2000;14:587-91.
27. Scheerlinck JPY, Snibson KJ, Bowles VM, Sutton P. Biomedical applications of sheep models: from asthma to vaccines. Trends Biotechnol 2008;26:259-66.
28. Xavier RG, Sanches PRS, Viera de Macedo Neto A, et al. Development of a modified Dumon stent for tracheal applications: an experimental study in dogs. J Bras Pneumol 2008;34:21-6.
29. Jung HS, Chae G, Kim JH, et al. Newly developed silicone airway stent (GINA stent): Mechanical characteristics and performance evaluation in pigs. bioRxiv 2020. 2020.10. 24.343533.
30. Rodrigues OR, Minamoto H, Canzian M, et al. Biocompatibility of a new device of self-expandable covered and non-covered tracheal stent: comparative study in rats. Acta Cir Bras 2013;28:10-8.
31. Schleich S, Kronen P, Krivitsky A, et al. Effects of shape and structure of a new 3D-printed personalized bioresorbable tracheal stent on fit and biocompatibility in a rabbit model. PLoS One 2024;19:e0300847.
32. Chen S, Du T, Zhang H, et al. Advances in studies on tracheal stent design addressing the related complications. Mater Today Bio 2024;20:101263.
33. Wang S, Chen Z, Lin Q, et al. In vitro pharmacokinetics of sirolimus-coated stent for tracheal stenosis. Trop J Pharm Res 2017;16:2033-8.

34. Wang T, Zhang J, Wang J, et al., Paclitaxel drug-eluting tracheal stent could reduce granulation tissue formation in a canine model. Chin Med J 2016;129:2708-13.
35. Maity N, Mansour N, Chakraborty P, et al. A personalized multifunctional 3d printed shape memory-displaying, drug releasing tracheal stent. Adv Funct Mater 2021;31:2108436.
36. Baskaran R, Ko UJ, Davaa E, et al. Doxycycline-eluting core-shell type nanofiber-covered trachea stent for inhibition of cellular metalloproteinase and its related fibrotic stenosis. Pharmaceutics 2019;11:421.
37. Zhao Y, Tian C, Wu K, et al. Vancomycin-loaded polycaprolactone electrospinning nanofibers modulate the airway interfaces to restrain tracheal stenosis. Front Bioeng Biotechnol 2021;9:760395.
38. Ke M, Zeng J, Chen Z, et al. Stent loaded with radioactive Iodine-125 seeds for adenoid cystic carcinoma of central airway: a case report of innovative brachytherapy. Front Oncol 2023;13:837394.
39. Stehlik L, Hytych V, Letackova J, et al. Biodegradable polydioxanone stents in the treatment of adult patients with tracheal narrowing. BMC Pulm Med 2015;15:164.
40. Liu CS, Feng BW, He SR, et al. Preparation and evaluation of a silk fibroin–polycaprolactone biodegradable biomimetic tracheal scaffold. J Biomed Mater Res B Appl Biomater 2022;110:1292-305.
41. Schopf LF, Fraga JC, Porto R, et al. Experimental use of new absorbable tracheal stent. J Pediatr Surg 2018;53:1305-9.
42. Xue B, Liang B, Yuan G, et al. A pilot study of a novel biodegradable magnesium alloy airway stent in a rabbit model. Int J Pediatr Otorhinolaryngol 2019;117:88-95.
43. Guibert N, Didier A, Moreno B, et al. Treatment of post-transplant complex airway stenosis with a three-dimensional, computer-assisted customized airway stent. Am J Respir Crit Care Med 2017;195:e31-3.

Online supplementary material
Supplementary Table 1. Scoring system for clinical tolerance.
Supplementary Table 2. Scoring of histological findings for tissue reactions and biocompatibility.

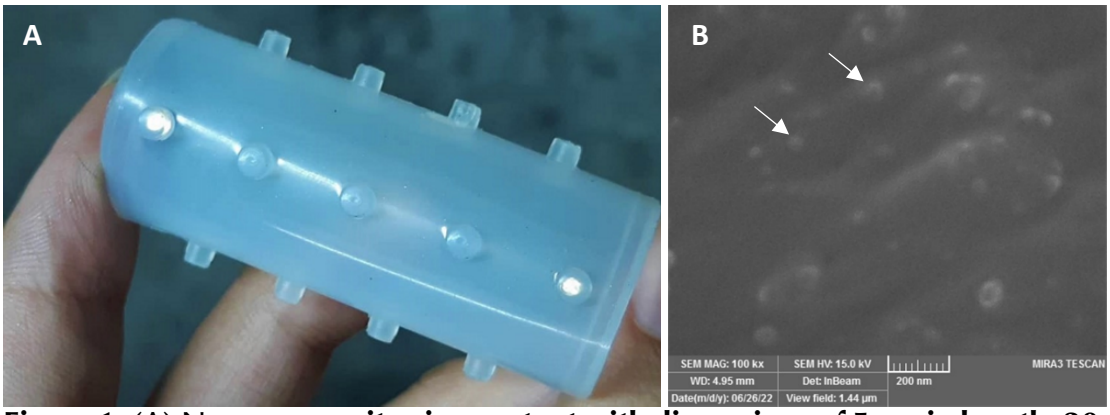

Figure 1. (A) Nanocomposite airway stent with dimensions of 5 cm in length, 20 mm in diameter, and 1.5 mm in thickness, (B) SEM image of stent nanostructure at ×100k magnification (View field: 1.44 µm, Scale bar = 200 nm) with accelerating voltage of 15.0 kV, demonstrating the silica nanoparticles as small, bright, and roughly spherical particles (white arrows) scattered across the field of view, which are uniformly distributed and well-separated, with minimal aggregation throughout the silicone matrix.

Figure 2. (A) Sheep were used during the anesthesia procedure, (B) the surgical team and the animal surgery room, (C) assembly of two endotracheal tubes, (D) endotracheal tube and silicone stent, and the balloon, (E) assembly of Ambu, the endotracheal tube, and stent.

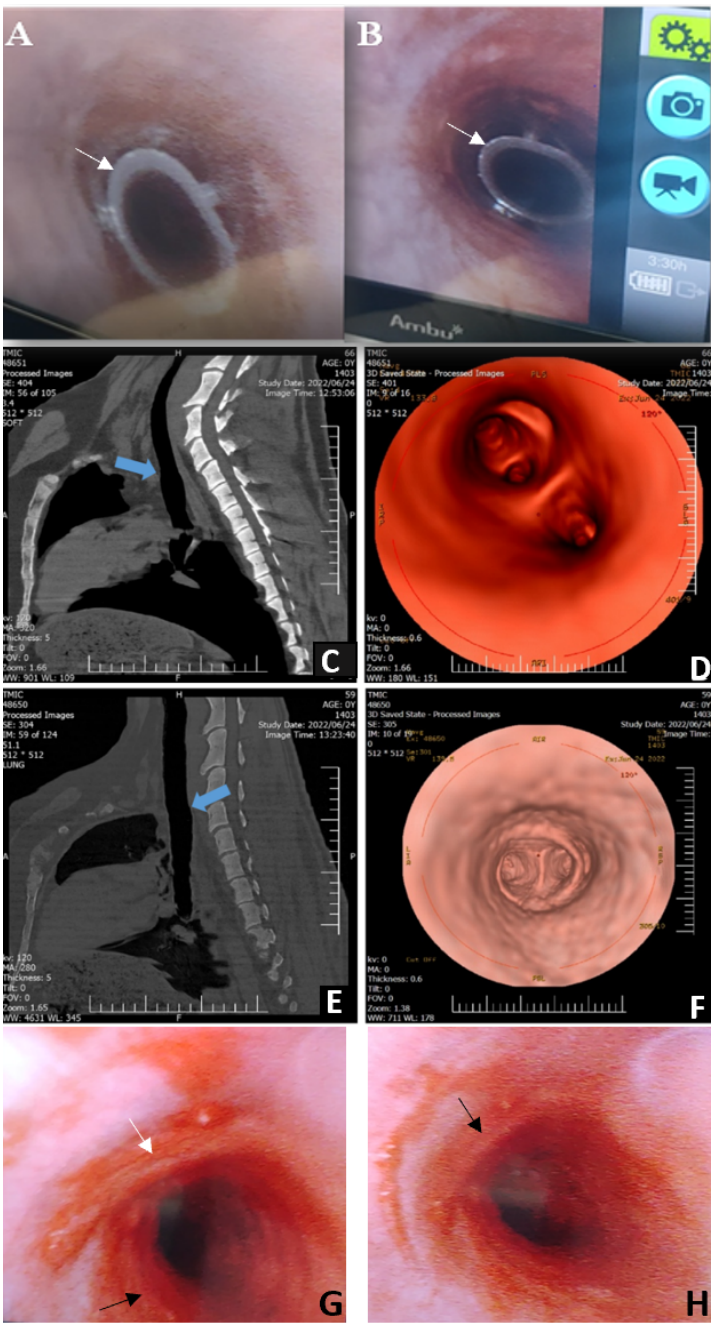

Figure 3. Immediate bronchoscopy of the stent (white arrows) after stenting, demonstrating proper stent positioning and well-placed to the tracheal wall for (A) sheep No.1 and (B) sheep No.2; (C, E) 3D Virtual Bronchoscopy of a silicone airway stent in the trachea; (D, F) A CT scan of the chest reveals a linear radiolucent structure within the trachea at the level indicated by the blue arrow, corresponding to the location of the nanocomposite silicon airway stent. VB shows that the silicon airway stent is appropriately placed in the trachea. The stent effectively restores airway patency, with no visible signs of migration, tracheal obstruction, or associated mucosal overgrowth or irregularity at the time of imaging. (C and D) for sheep No.1 and (E and F) for sheep No.2; (G, H) Bronchoscopy shows the stent site after two-month follow-up, demonstration superficial erosions with irregular red borders are on the mucosal surface around the lumen, caused by friction or pressure from the stent for (G) sheep No.1 and (H) sheep No.2. These erosions (black arrows) and the biopsy site (white arrow) are labeled in the figure.

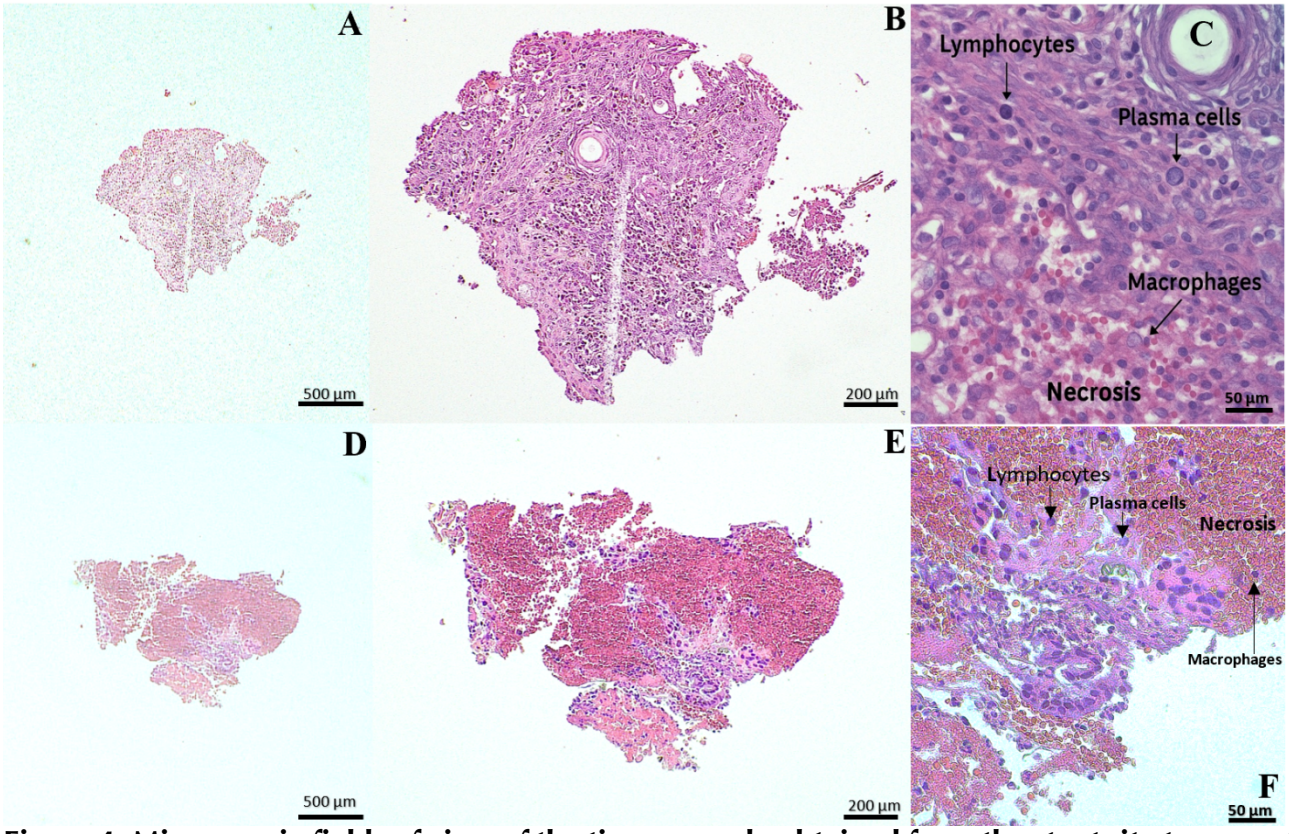

Figure 4. Microscopic fields of view of the tissue sample obtained from the stent site two months post-procedure of sheep No.1 (A,B,C) and sheep No.2 (D,E,F), (A,D) ×4 magnification (Scale bar = 500 µm), (B,E) ×10 magnification (Scale bar = 200 µm), (C,F) ×40 magnification (Scale bar = 50 µm). Lymphocytes, plasma cells, macrophages, and necrosis are labeled with arrows in the field (C).